

CONTRIBUTION THE DEVELOPMENT OF METHODOLOGY FOR ASSESSING THE IMPACT OF BUS SUSPENSION SYSTEM ON FUEL CONSUMPTION AND CO₂ EMISSION

by

**Dragan S. SEKULIĆ, Ivan S. IVKOVIĆ*, Dušan M. MLADENović,
and Davor B. VUJANOVIĆ**

Faculty of Transport and Traffic Engineering, University of Belgrade, Belgrade, Serbia

Original scientific paper

<https://doi.org/10.2298/TSCI191224168S>

This paper analyzes the effects of intercity bus suspension system oscillatory parameters on driver's ride comfort and road damage. The analysis has been carried out through simulation by means of validated in-plane bus model with six degrees of freedom excited by real road roughness signal. Low root-mean-square values of the weighted vertical acceleration (less than 0.315 m/s²) have been achieved by shock-absorbers with lower damping coefficient and softer suspension system springs. Low values of dynamic load coefficient provide low shock-absorber damping and softer springs. However, low crest factor values for both axles are accomplished for high shock-absorber damping and softer springs in bus suspension system. Results from this analysis could be used as reference for selecting proper oscillatory parameter values when designing road-friendly bus suspension system which in turn would increase vehicle energy efficiency. Presented methods, results and analyzes are the part of wider methodology for assessing the impact of bus suspension system on fuel consumption and CO₂ emission.

Key words: bus, suspension system, energy efficiency, oscillatory comfort, road damage, CO₂ emission, fuel consumption, simulation

Introduction

Oscillatory movements have negative influence on bus users and road. Some of the negative influences are decrease in comfort and working ability of driver and passengers. Reducing of driver's comfort and his working ability negatively affect the fuel consumption, energy efficiency of the vehicle, transport and vehicle maintenance costs [1]. In addition, CO₂ emission increases proportionally with the increase in fuel consumption [2]. Bus oscillatory movements relate to appearance of dynamic tire forces which cause road load and road construction damage, e.g. crack caused by fatigue, permanent deformation, etc. These road damages cause a change in the pavement texture (macro/micro road roughness), and increase in both – rolling resistance and the international roughness index (IRI). Many studies have shown that pavement damages cause increase of fuel consumption, and thus increase of CO₂ emission. For example, a linear dependency between the coefficient of rolling resistance and fuel consumption was shown in [3]. Fuel consumption increases by around 15% if the coefficient of rolling resistance increases from 0.010-0.020 [3]. Van Dam *at al.* [4] shows the significant impact of different measured values of IRI on fuel economy. Zaabar and Chatti [5] presents percentage

* Corresponding author, e-mail: i.ivkovic@sf.bg.ac.rs

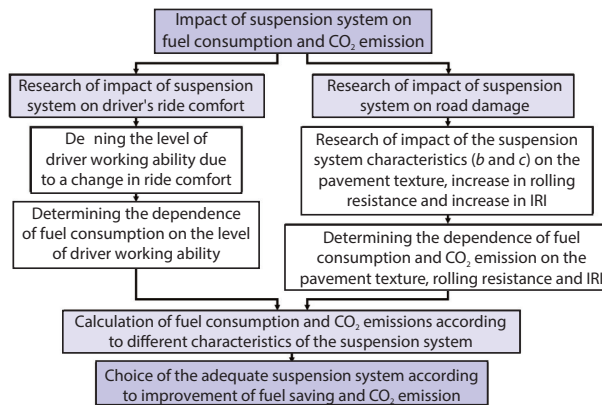


Figure 1. Methodological approach for assessing the impact of a vehicle suspension system on fuel consumption and CO₂ emission

the vehicle suspension system on fuel consumption and CO₂ emission, the indispensable step is to analyze the impact of the suspension system oscillatory parameters on road damage and driver's comfort.

According to Potter *et al.* [7], dynamic wheel load (DWL) causes rapid and premature road damage. Dynamic load coefficient (DLC), and crest factor (CF), are frequently used measures when assessing potential road damage. The CF is used in the case of *spatial repeatability* loading [7-9]. The DWL in function of speed and road type for three different types of vehicle – car, bus, and truck have been analyzed in [10]. Agostinacchio *et al.* [10] concluded that heavy vehicles cause noticeable dynamic overload, especially in the cases when roughness irregularities increase. The damage of a semi rigid pavement under heavy vehicle loads with varied suspension/tire oscillatory parameters is studied in [11]. Xia *et al.* [11] reported that pavement dynamic stresses increase with increases in suspension/tire stiffness and decrease with increases in suspension/tire damping.

The aim of this research is to reveal the effects of the bus suspension system stiffness/damping coefficient values on the potential road damage and driver's ride comfort. The second aim is to reveal whether the oscillatory parameters that enable the most favourable driver's ride comfort also enable the most favourable DLC/CF values. The overall goal of this research is to propose recommendation for selecting bus suspension oscillatory parameters needed to reduce potential road damage and provide satisfactory ride comfort. The analysis has been carried out through simulation by means of in-plane intercity bus linear oscillatory model.

Bus oscillatory model

The effect of heavy vehicle roll-plane dynamics on ride comfort and DWL is insignificant for usual exploitation condition [12]. In-plane bus model with six DoF has been used in analysis, fig. 2. The DoF are vertical movement of the driver, z_d , seat, z_s , center of gravity, z , front and rear axle, z_{fa} and z_{ra} , as well as angle movement of sprung bus mass around y -axis, pitching, θ .

Intercity bus IK-301 has pneumatic suspension system with rigid axles [13]. The notations in fig. 2 and values of every parameter could be found in [14, 15]. Parameters and their values important for simulations done in this paper have been interpreted in tab. 1.

increase in fuel consumption in function of IRI values for different vehicle categories. If IRI increases from 1 to 5 m/km, fuel consumption increases by up to 5% [5]. Ivković *et al.* [6] presents the change in fuel consumption of different vehicle categories according to different vehicle speeds relative to different IRI values.

In order to determine the impact of the vehicle suspension system on fuel consumption and CO₂ emission, a complex methodological approach is necessary. Figure 1 presents basic steps of purposed methodological approach. According to fig. 1, it is clear that in assessing the impact of

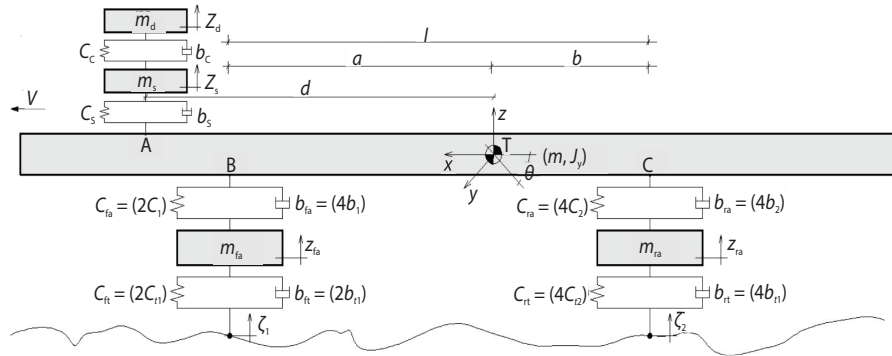


Figure 2. In-plane bus IK-301 oscillatory model

Table 1. Geometric, mass and oscillatory parameters of intercity bus IK-301

Wheelbase, l [m]	5.65	Front axle single air bag stiffness, c_1 [Nm^{-1}]	175000
Distance from front axle to center of gravity of loaded bus, a [m]	3.55	Front axle equivalent air bags stiffness, c_{fa} [Nm^{-1}]	350000
Distance from rear axle to center of gravity of loaded bus, b [m]	2.10	Front axle single shock-absorber damping, b_1 [Nsm^{-1}]	20000
Distance from the driver seat to bus center of gravity, d [m]	1.6	Front axle equivalent shock-absorber damping, b_{fa} [Nsm^{-1}]	80000
Sprung mass, m [kg]	15399	Rear axle single air bag stiffness, c_2 [Nm^{-1}]	200000
Front axle mass, m_{fa} [kg]	745.6	Rear axle equivalent air bags stiffness, c_{ra} [Nm^{-1}]	800000
Rear axle mass, m_{ra} [kg]	1355	Rear axle single shock-absorber damping, b_2 [Nsm^{-1}]	22500
Mass of the driver, m_d [kg]	70	Rear axle equivalent shock-absorber damping, b_{ra} [Nsm^{-1}]	90000
Mass of the seat, m_s [kg]	30	Single tyre stiffness on the front and the rear axle, c_{t1} [Nm^{-1}]	1000000
Suspended mass moment of inertia relative to the y -axis, J_y [kgm^2]	150000	Single tyre damping on the front and the rear axle, b_{t1} [Nsm^{-1}]	150
Seat cushion stiffness, c_c [Nm^{-1}]	20000	Equivalent tyre stiffness for the front axle, c_{ft} [Nsm^{-1}]	2000000
Seat cushion damping, b_c [Nsm^{-1}]	200	Equivalent tyre damping for the front axle, b_{ft} [Nsm^{-1}]	300
Spring stiffness of the driver seat suspension system, c_s [Nm^{-1}]	5000	Equivalent tyre stiffness for the rear axle, c_{rt} [Nsm^{-1}]	4000000
Shock-absorber damping of the driver seat suspension system, b_s [Nsm^{-1}]	900	Equivalent tyre damping for the rear axle, b_{rt} [Nsm^{-1}]	600

Values of equivalent stiffness and equivalent damping for front and rear axle in the range of $\pm 50\%$ of their equivalent nominal values have been shown in tab. 2. Oscillatory parameter values from tab. 2 have been considered while performing the simulations.

Table 2. Range of considered values of suspension system oscillatory parameters used in simulation

	-50%	-25%	Nominal value	+25%	+50%
Front axle stiffness [Nm ⁻¹]	175000	262500	350000	437500	525000
Front axle damping [Nsm ⁻¹]	40000	80000	80000	100,000	120,000
Rear axle stiffness [Nm ⁻¹]	400000	600000	800000	1000000	1200000
Rear axle damping [Nsm ⁻¹]	45000	90000	90000	112500	135000

Applying Lagrange's equations of the second kind, the differential equations of motion are obtained:

$$m_d \ddot{z}_d + b_c \dot{z}_d + c_c z_d - b_c \dot{z}_s - c_c z_s = 0 \quad (1)$$

$$m_s \ddot{z}_s + (b_c + b_s) \dot{z}_s + (c_c + c_s) z_s - b_c \dot{z}_d - c_c z_d - b_s \dot{z} - c_s z - b_s d \dot{\theta} - c_s d \theta = 0 \quad (2)$$

$$m \ddot{z} + (b_s + b_{fa} + b_{ra}) \dot{z} + (c_s + c_{fa} + c_{ra}) z + (db_s + ab_{fa} - bb_{ra}) \dot{\theta} + (dc_s + ac_{fa} - bc_{ra}) \theta - b_s \dot{z}_s - c_s z_s - b_{fa} \dot{z}_{fa} - c_{fa} z_{fa} - b_{ra} \dot{z}_{ra} - c_{ra} z_{ra} = 0 \quad (3)$$

$$J_y \ddot{\theta} + (d^2 b_s + a^2 b_{fa} + b^2 b_{ra}) \dot{\theta} + (d^2 c_s + a^2 c_{fa} + b^2 c_{ra}) \theta - db_s \dot{z}_s - dc_s z_s + (db_s + ab_{fa} - bb_{ra}) \dot{z} + (dc_s + ac_{fa} - bc_{ra}) z - ab_{fa} \dot{z}_{fa} - ac_{fa} z_{fa} + bb_{ra} \dot{z}_{ra} + bc_{ra} z_{ra} = 0 \quad (4)$$

$$m_{fa} \ddot{z}_{fa} + (b_{fa} + b_{ft}) \dot{z}_{fa} + (c_{fa} + c_{ft}) z_{fa} - b_{fa} \dot{z} - c_{fa} z - ab_{fa} \dot{\theta} - ac_{fa} \theta = b_{ft} \zeta_1 + c_{ft} \zeta_1 \quad (5)$$

$$m_{ra} \ddot{z}_{ra} + (b_{ra} + b_{rt}) \dot{z}_{ra} + (c_{ra} + c_{rt}) z_{ra} - b_{ra} \dot{z} - c_{ra} z + bb_{ra} \dot{\theta} + bc_{ra} \theta = b_{rt} \zeta_2 + c_{rt} \zeta_2 \quad (6)$$

Based on differential equations of motion, block diagram has been formed in MATLAB/SIMULINK software. The MATLAB built-in function ode45 has been used for solving differential equations of motion. Defined starting conditions for each variable are set to zero. Time period chosen for simulation is 7 seconds.

Bus excitement

The power spectral densities (PSD) functions of road elevation have been broadly used for numerical simulation of road irregularities [10, 16-18]. However, in this research real road roughness was considered [19]. Law profiler recorded road roughnesses along two tracks at speed of 80 km/h, fig. 3(a). It could be noticed that the road profile has localized bump around 4 cm high on 80 m of the longitudinal distance, fig. 3(a). According to [8], DWL due to localized bumps have the most significant influence on road damage.

Maximal values of DWL caused by localized bumps have 1.5-12 times greater effect on road damage in comparison with damage caused by static wheel load [8]. In this paper the effects of localized bump on road damage is considered through CF value. Short wavelengths irregularities (up to 0.3 m) are filtered by heavy vehicles tires [12]. Irregularities with long wavelengths indicate the longitudinal road profile character and do not have significant influence on vehicle's oscillatory movement. Frequencies excitation range 1-30 Hz affect vehicle oscillatory behaviour the most [20]. The connection between irregularities wavelength, vehicle speed and road excitation frequency can be represented:

$$\lambda = \frac{V}{f} \quad (7)$$

where λ is irregularities wavelength, V – the vehicle speed, and f – the road excitation frequency. Excitation frequency range, for vehicle speed of 80 km/h, corresponds with wavelength irregularities range 44.44-0.74 m. Having this in mind, road roughness signals were filtered using moving average band-pass filter in engineering software application ProVal 3.6 [21]. For the speed of 80 km/h, frequency range 1.5-4 Hz corresponds with wavelength irregularities range 14.8-5.55 m. Frequency range 8-15 Hz corresponds with wavelength irregularities range 2.77-1.48 m. Roughness irregularities important for excitation of the sprung and un-sprung bus masses vibration modes have been covered by bus excitation wavelength range.

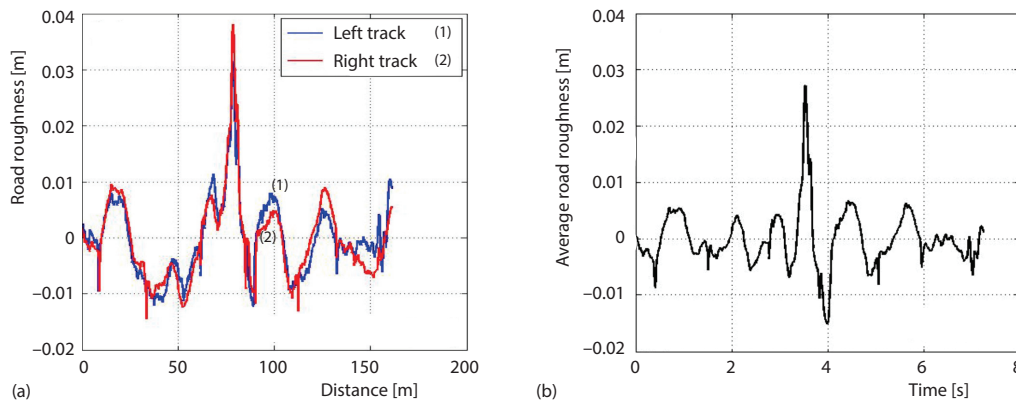


Figure 3. Roughness of good asphalt-concrete road; (a) left/right track and (b) averaged track

Averaged roughness, after filtering roughness on left and right tracks, in function of time has been shown in the fig. 3(b). This excitation signal has been introduced in the in-plane oscillatory bus model.

Oscillatory model validation

Bus model was validated by three different oscillatory quantities: vertical acceleration on the driver seat surface and vertical accelerations on the front/rear bus axles. The measurements of these quantities were carried out on the empty intercity bus IK-301 on two different sections of the Airport-Ikarbus asphalt-concrete road in a good condition [14]. Bus was moving at speed of 80 km/h. Driver, one passenger and two persons for data collection participated in the measurements [14]. The first measurement (MEASUREMENT 4) registered vertical accelerations on the front bus axle left/right side with the accelerometer placed near to the airbag, fig. 4(b). The first measurement also registered the acceleration signal below the driver's body on his seat, fig. 5(a). Acceleration signals on both axle sides were similar in terms of their tendency change and values. Vertical acceleration on the front axle left side is presented in fig. 5(b). The second measurement (MEASUREMENT 13) registered the acceleration signals on rear bus axle left/right side. Vertical acceleration on the rear axle left side is presented in fig. 5(c). WBV tri-axial seat pad accelerometer (B&K type 4321) was used for driver's acceleration signal recording, fig. 4(a). An amplifier B&K type 2639 was used to amplify the output signal from the accelerometer. Axles' vertical acceleration signals were registered by inductive accelerometer HBM type B12/200, fig. 4(b). Signals were recorded during 13.65 seconds.

Figure 5 show vertical acceleration signals on the driver's seat surface and on bus front/rear axles determined by measurements and simulation. With the fig. 5(a), the acceleration of 10 m/s^2 corresponds to the voltage of 1 V.

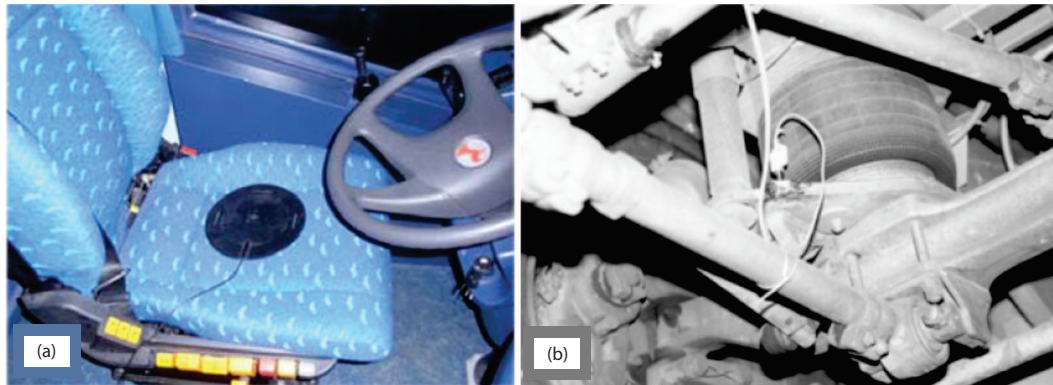


Figure 4. Accelerometers for acceleration recording on (a) driver's seat and (b) bus axle

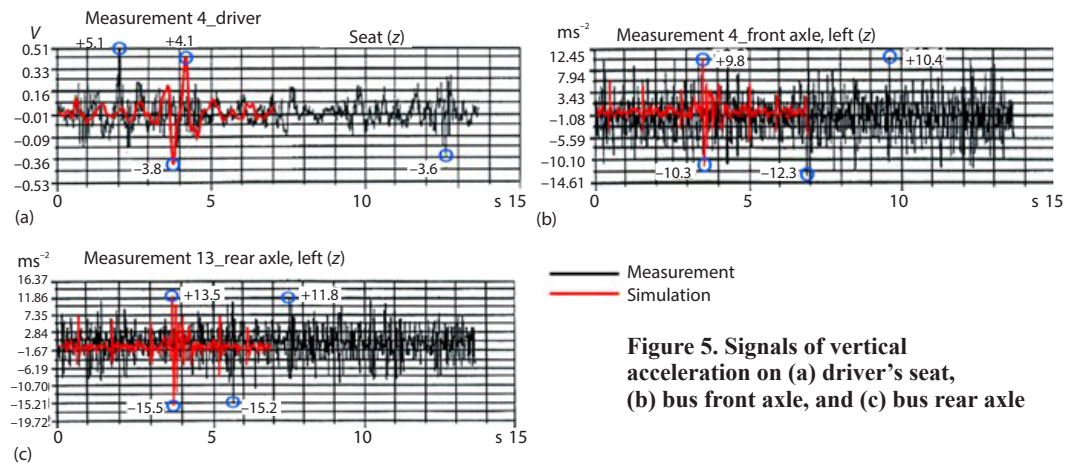


Figure 5. Signals of vertical acceleration on (a) driver's seat, (b) bus front axle, and (c) bus rear axle

Table 3 gives values of statistical parameters (maximum, minimum, mean value and dispersion) obtained by measurements and simulation. It could be noticed that statistical values slightly differ for simulation and experimental data. Measured and simulated acceleration signals are similar in their magnitudes, but with some differences in their frequencies, fig. 5. The results show correlation, although the acceleration signal is registered on the road section of the

Table 3. Values of statistical parameters for vertical accelerations established by measurements and simulation

Statistical parameters	Driver		Front axle		Rear axle	
	Measurement	Simulation	Measurement	Simulation	Measurement	Simulation
Maximum value	5.10	4.0795	10.40	9.7587	11.76	13.5496
Minimum value	-3.60	-3.8392	-12.32	-10.2661	-15.21	-15.4863
Mean value	0.00	-0.0031	-0.04	-0.0072	0.03	-0.0052
Dispersion	0.90	0.8602	2.61	1.8208	5.13	3.7109
Standard deviation	0.9487	0.92746	–	–	–	–
Root mean square (RMS) value	0.9487	0.92747	–	–	–	–

same type and condition but not on the same location. Besides the road excitations differences, some simplifications referring to bus oscillatory model might affect simulation results (such as using in-plane and not space bus model, linear characteristics of elastic/damper elements, point wheel-road contact, *etc.*).

Simulation results and discussion

Driver's ride comfort assessment is made through procedures prescribed by the ISO 2631/1997 standard [22]. Assessing the effect of wheel tire forces on road damage is made by using two quantities – DLC and CF. The simulation has been done in such a way that the equivalent coefficient values of oscillatory parameters have simultaneously been changing on both axles suspension system.

The effect of oscillatory parameters on driver's oscillatory comfort

Driver's vertical acceleration for different values of spring stiffness and nominal value of the shock-absorber damping coefficient is shown in fig. 6(a). With softer springs vertical accelerations values are lower intensities, especially peak acceleration values, around 4 seconds from the beginning of simulation. This moment corresponds the bus passing over the 4 cm high localized bump, as shown in fig. 3(a). Figures 6(b) provides the change of driver's vertical acceleration in function of shock-absorber damping for nominal value of spring stiffness coefficient. It could be observed that the lower values of shock-absorber damping provide lower values of vertical accelerations.

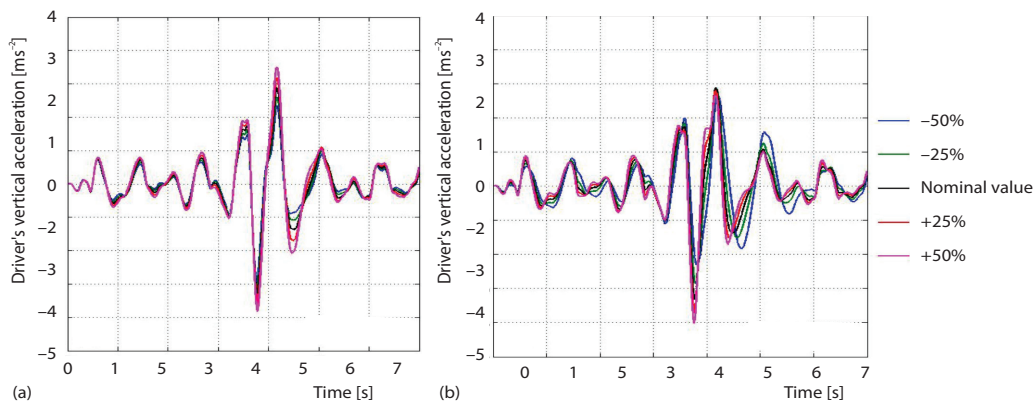


Figure 6. Driver's vertical acceleration for (a) nominal damping coefficient value and different stiffness values and (b) nominal stiffness coefficient value and different damping values, tab. 2

Figure 7. Constrained forces for nominal damping coefficient value and different stiffness values

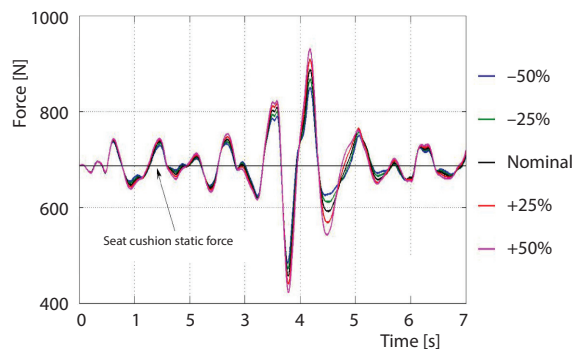


Figure 7 shows constrained forces between driver's body and seat in function of time. The forces had positive values, meaning that contact had not been lost. Permanent contact between driver's body and his seat was a prerequisite for using the differential equations of motion, eq. (1)-(6).

Figure 8 shows PSD of vertical accelerations acting on driver's body. The PSD were obtained according to the Welch method implemented by the *pwelch* function in the MATLAB signal processing toolbox. Vibration intensities were distributed in the frequency range 0-4 Hz. The seat attenuated vertical vibrations at frequencies above 4 Hz. The maximum values of PSD were around 2 Hz which corresponds to resonant frequency of the bus driver's seat [15]. With the increase of spring stiffness, amplitudes of vertical vibrations increase in frequency range 0-2 Hz, fig. 8(a). With the increase in damping, amplitudes of vertical vibrations slightly increase in frequency range 2-4 Hz, fig. 8(b).

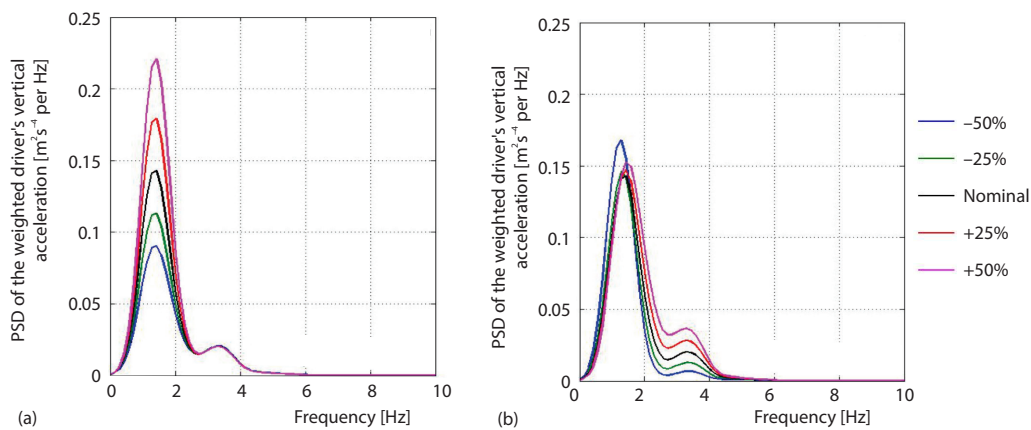


Figure 8. The PSD of driver's vertical acceleration for (a) nominal damping coefficient value and different stiffness values and (b) nominal stiffness coefficient value and different damping values, tab. 2

Weighted RMS values of driver's vertical accelerations and comfort assessment in function of stiffness and damping are shown in tab. 4. It can be noticed that weighted RMS acceleration increases as spring stiffness increases. With springs of the highest stiffness (+50% of nominal value) acceleration exceeds 0.5 m/s^2 , so the driver's comfort assessment is *fairly uncomfortable*. With the increase of damping, weighted accelerations also increase, but the acceleration change is less prominent in comparison with change due to spring stiffness. When the stiffness increases for 50%, acceleration increases for 18.40%. If there is 50% increase in damping, acceleration increases for 12.26%. For the entire range of considered damping values, weighted RMS acceleration is less than 0.5 m/s^2 , so that driver's comfort assessment is *little uncomfortable*.

Dependency of RMS of the weighted driver's vertical acceleration as a function of spring stiffness and the shock-absorber damping coefficient is shown in the fig. 9. Low values (less than 0.315 m/s^2) are accomplished by lower shock-absorber damping and low spring stiffness values. With the rise of stiffness for all damping values, RMS of the weighted acceleration rises. For low shock-absorber damping coefficient (-50% of nominal value) and high spring stiffness coefficient (+50% of nominal value), RMS of the weighted acceleration reaches the highest value (approximately 0.6 m/s^2). Vehicle providing good ride comfort positively affects driver's working ability which results in lowering fuel consumption and apparently in increasing energy efficiency [1].

Table 4. Weighted RMS values of driver’s vertical accelerations and ride comfort assessment according to ISO 2631/1997

Stiffness [Nm ⁻¹]	Weighted RMS vertical acceleration [ms ⁻²]	Comfort assessment [ISO 2631/1997]	Damping [Nsm ⁻¹]	Weighted RMS vertical acceleration [ms ⁻²]	Comfort assessment [ISO 2631/1997]
-50%	0.362	Little uncomfortable	-50%	0.409	Little uncomfortable
-25%	0.391	Little uncomfortable	-25%	0.406	Little uncomfortable
Nominal value	0.418	Little uncomfortable	Nominal value	0.418	Little uncomfortable
+25%	0.462	Little uncomfortable	+25%	0.450	Little uncomfortable
+50%	0.502	Fairly uncomfortable	+50%	0.476	Little uncomfortable

The perception of user’s comfort in public transport for different vibration intensity according to ISO 2631/1997 is shown in tab. 5.

Figure 9. The RMS of the weighted driver’s vertical acceleration as a function of spring stiffness and shock-absorber damping

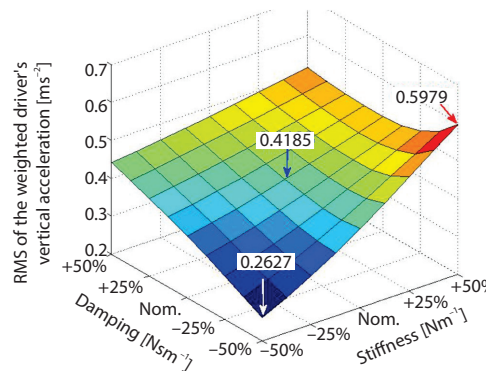


Table 5. Comfort criteria in means of public transport for different acceleration values, (ISO 2631/1997)

	Comfort assessment					
	Comfortable	Little uncomfortable	Fairly uncomfortable	Uncomfortable	Very uncomfortable	Extremely uncomfortable
Vibration intensity [ms ⁻²]	< 0.315	0.315-0.63	0.5-1	0.8-1.6	1.25-2.5	> 2

The effect of oscillatory parameters on road damage

Total bus axle load is comprised of static and dynamic part:

$$Z(t) = Z_{st} + Z_{dyn}(t) \tag{8}$$

where Z_{st} is static axle load and $Z_{dyn}(t)$ is dynamic axle load. Dynamic part could have positive and negative values. Total axle loads is equal to zero when $Z_{dyn}(t) = -Z_{st}$ and there has been a loss of contact between the wheel and the road surface.

As an example, the total front and rear bus axle loads for different shock-absorber damping values and nominal value of the spring stiffness coefficient are shown in the fig. 10. The highest values of total loads for both bus axles have been accomplished approximately 4 seconds after the beginning of simulation which corresponds to the moment when the bus crossed over the localized 4 cm high bump.

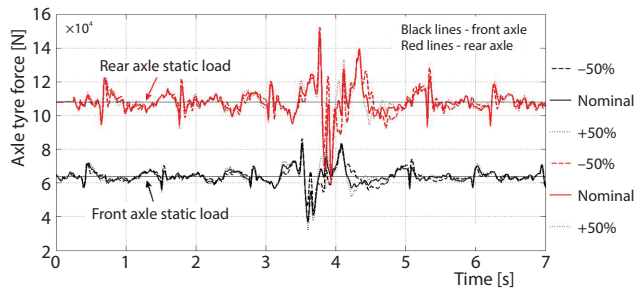


Figure 10. Front and rear bus axle tyre forces for different shock-absorber damping values and nominal spring stiffness value, tab. 2

Figure 11(a) displays PSD of dynamic axles load in the functions of spring stiffness for nominal value of shock-absorber damping coefficient. It is noticed that the change of spectral densities is the most prominent for low excitation frequencies. With the increase of spring stiffness, amplitudes of dynamic load for both axles increase in the excitation frequency range close to the resonant frequency of the bus body, around 1.5 Hz. For excitation frequencies close to the resonant frequency of the bus axles (around 9 Hz), amplitudes of dynamic rear axle loads decreased by little with the increase in spring stiffness. The change in stiffness does not affect the change of dynamic front axle loads amplitudes for excitation frequencies around 9 Hz. Low stiffness springs provide lower dynamic axle loads, and apparently less road damage. Figure 11(b) shows PSD of dynamic axles load in the functions of shock-absorber damping for nominal value of spring stiffness coefficient. It should be noticed that the change of damping has most effect on the amplitude change for dynamic rear axle load. Shock-absorber with higher damping coefficient provides lower values of PSD dynamic load for rear axle for the excitation frequencies close to resonant frequencies of the bus body and bus axles. The opposite applies for the frequency range of approximately 2-7 Hz.

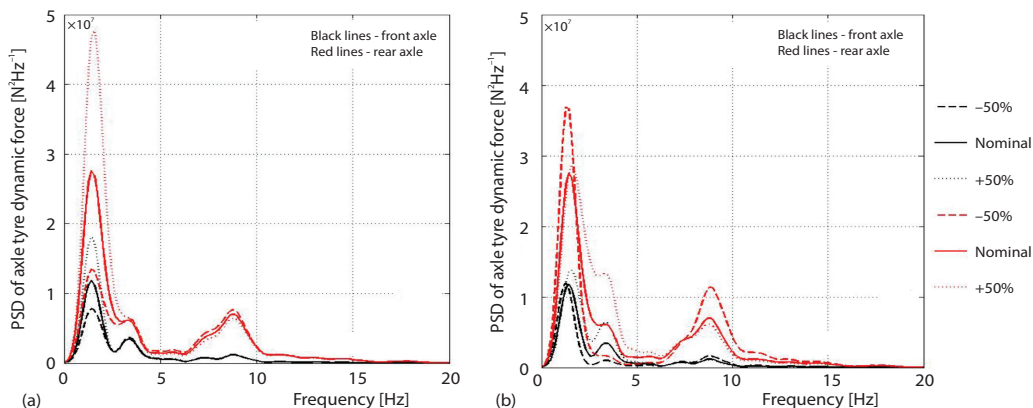


Figure 11. The PSD of dynamic axle load for (a) nominal damping coefficient value and different stiffness values and (b) nominal stiffness coefficient value and different damping values, tab. 2

The PSD amplitudes of dynamic axles load are concentrated in two distinct frequency ranges corresponding to sprung and un-sprung bus masses vibration modes. These characteristics for heavy vehicles have been confirmed by various theoretical/experimental studies presented in [8]. Intensities of DWL usually dominate in the lower frequency range when heavy vehicle is moving on good quality roads [8].

Dynamic load coefficient and crest factor

The DLC represents ratio of standard deviation of total axle load (or RMS value of dynamic axle load) and static axle load:

$$DLC = \frac{\sigma_z}{Z_{st}} = \frac{Z_{din,eff}}{Z_{st}} \tag{9}$$

where σ_z is standard deviation of total axle load and $Z_{din,eff}$ is RMS value of dynamic axle load. The value of DLC, under normal condition of heavy vehicles exploitation, is in the range from 0.05 to 0.3 [23, 24]. Value of 0.4 points the loss of contact between the wheels and the road surface during the vehicle exploitation, and as a result greater road damage. Lower values of this parameter point to the smaller changes in dynamic axle load and therefore, minor road damage. For very flat and smooth surfaces, value of this factor is close to zero. For surfaces in reasonably good condition the DLC value is approximately up to 8% [12]. The DLC is, according to in-plane oscillatory model, determined for front and rear bus axles. Table 6 shows calculated coefficient values for both axles in function of spring stiffness and shock-absorber damping. It could be observed that when spring stiffness increases the both axles' coefficient values increase as well. The lowest coefficient value on rear axle of 0.069 is accomplished by shock-absorber damping of -25% of its nominal value. Calculated DLC values are in the range of approximately 0.06-0.085 which is expected for the bus moving on good quality asphalt-concrete road.

Table 6. Calculated DLC values in function of spring stiffness and shock-absorber damping

		Stiffness [Nm ⁻¹]					Damping [Nsm ⁻¹]				
		-50%	-25%	Nominal value	+25%	+50%	-50%	-25%	Nominal value	+25%	+50%
DLC [-]	Front axle	0.068	0.070	0.074	0.078	0.082	0.067	0.069	0.074	0.079	0.084
	Rear axle	0.062	0.065	0.070	0.075	0.081	0.074	0.069	0.070	0.073	0.077

Figure 12 shows dependency of DLC in function of spring stiffness and shock-absorber damping for front and rear bus axles. Low coefficient values are accomplished by low levels of shock-absorber damping and softer springs in bus suspension system. With axle springs of higher stiffness, when damping increase, DLC value declines at first and then increases. For low damping and high stiffness, the highest calculated value of this coefficient on both axles is approximately 0.09.

The CF is defined as ratio of total axle load maximal value and axle load static value is given:

$$CF = \frac{Z_{max}}{Z_{st}} \tag{10}$$

where Z_{max} is maximal value of the total axle load. This factor is good indicator for assessing road damage potential of the bus if the maximal values of dynamic load are concentrated in proximity of localized road bumps (*i.e.* scenario of spatially repeatable loading). Table 7 shows calculated CF values. It can be noticed that CF values on both axles increase as spring stiffness increases.

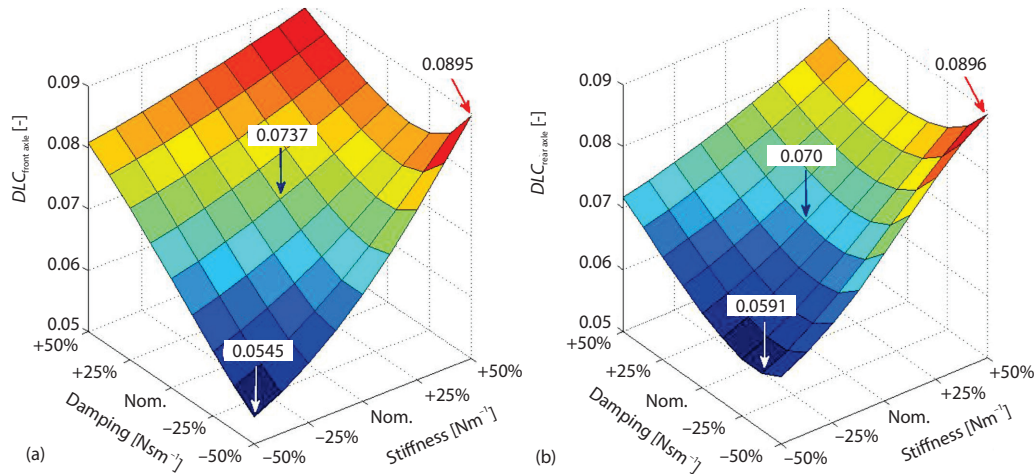


Figure 12. Change of DLC value in function of spring stiffness and shock-absorber damping for (a) front axle and (b) rear axle

For the entire range of the stiffness coefficient value, higher CF values are realized on the bus rear axle. When shock-absorber damping increases the CF values decrease for both axles. For the entire range of damping coefficient value, higher CF values are realized on the bus rear axle.

Table 7. Calculated CF values in function of spring stiffness and shock-absorber damping

		Stiffness [Nm ⁻¹]					Damping [Nsm ⁻¹]				
		-50%	-25%	Nominal value	+25%	+50%	-50%	-25%	Nominal value	+25%	+50%
CF [-]	Front axle	1.293	1.299	1.310	1.327	1.344	1.354	1.326	1.310	1.306	1.298
	Rear axle	1.364	1.374	1.381	1.383	1.382	1.410	1.395	1.381	1.369	1.359

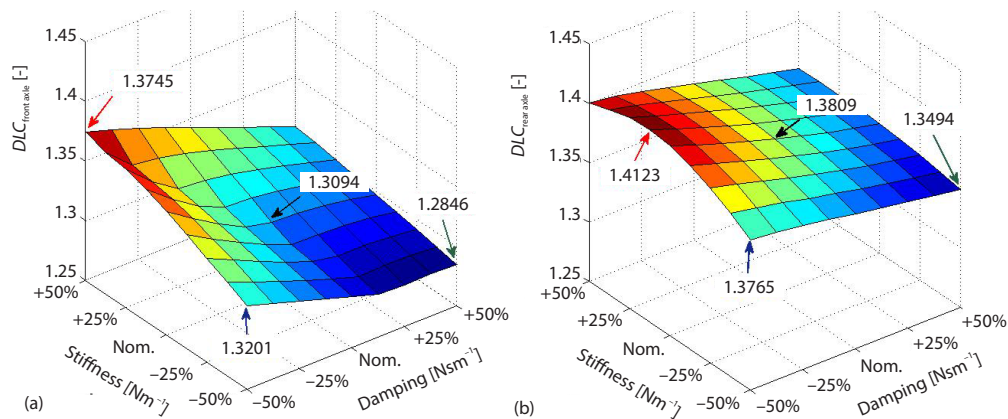


Figure 13. Change of CF value in function of spring stiffness and shock-absorber damping for (a) front axle and (b) rear axle

Change of CF in function of spring stiffness and shock-absorber damping coefficient is shown in the fig. 13. It could be seen that higher CF values are prominent on the rear bus axle. Low factor values for both axles have been accomplished in case of high shock-absorber

damping and softer springs in the bus suspension system. For damping of +50% and spring stiffness of –50% of their nominal values, the lowest CF values for the front and rear axle have been achieved (1.29 and 1.35, respectively).

It should be noticed that CF value on front axle for damping/stiffness of –50% of their nominal values is a little over from CF value corresponding to damping/stiffness nominal values. Opposite is true for CF value on bus rear axle.

Conclusions

In this research paper in-plane oscillatory model of intercity bus with six DoF has been defined. Oscillatory model is verified by three different vertical acceleration signals and important statistical parameters. Analysis on effect of suspension system oscillatory parameters on potential road damage and driver's oscillatory comfort has been carried out. Real asphalt-concrete road excitation in good condition registered at 80 km/h speed is introduced in the bus model. The main conclusions follow from this research.

- With lower shock-absorber damping and lower spring stiffness in the bus suspension system, more desirable weighted driver's vertical accelerations values have been accomplished (RMS value lower than 0.315 m/s^2). With increase of spring stiffness for all damping values, weighted RMS acceleration increases. The effect of stiffness on RMS weighted acceleration change is more prominent in comparison with the effect of shock-absorber damping.
- The PSD amplitudes of dynamic axles load are concentrated in two distinct frequency ranges corresponding to sprung and un-sprung bus masses vibration modes. Higher intensities of dynamic axle load, when both spring stiffness and shock-absorber damping change, are in the lower excitation frequencies (around 1.5 Hz).
- Calculated values of DLC are in the range from 0.06-0.085 and correspond to usual DLC values for good quality road surfaces. Low DLC values are accomplished by low levels of shock-absorber damping and softer spring in the bus suspension system. With axle springs of higher stiffness, when shock-absorber damping coefficient increases, DLC value declines at first and then increases.
- Low CF values, unlike to DLC, are accomplished for high shock-absorber damping and softer springs in the bus suspension system. For shock-absorber damping of +50% and spring stiffness of –50% of their nominal values, the lowest CF values for both bus axles have been achieved.
- The most favourable values for DLC and CF could not be achieved with the same values of the suspension stiffness and damping coefficients.
- The most favourable values for both DLC and weighted RMS vertical acceleration could be achieved with the same stiffness/damping coefficients values. However, it is not the case for CF and weighted RMS driver's vertical acceleration.
- The CF are higher values on the rear bus axle. The CF value on rear axle for the lowest damping/stiffness coefficients is lower than CF value corresponding to damping/stiffness coefficient nominal values. Consequently, taking into consideration two different criteria (DLC and CF) and weighted RMS vertical acceleration value, lower suspension stiffness/damping coefficients enable reduction in potential road damage as well as better bus ride comfort. Ride comfort improvement would enable better driver's working ability and energy efficiency of the bus.

Results presented in this paper should be considered as the basic for assessing the impact of the bus suspension system on fuel consumption and CO₂ emission. With vehicle model calibration and appropriate input data, it is possible to implement purposed methodological approach on the other vehicle categories.

Acknowledgment

Support for this research was provided by the Ministry of Education, Science and Technological Development of the Republic of Serbia (Grant No. TR36027).

Nomenclature

a, b	– distance from front/rear axle to center of gravity of loaded bus, [m]	J_y	– suspended mass moment of inertia relative to the y -axis, [kgm^2]
b_1, b_2	– front and rear axle single shock-absorber damping, [Nsm^{-1}]	l	– wheelbase, [m]
b_c	– seat cushion damping, [Nsm^{-1}]	m	– sprung mass, [kg]
b_{fa}, b_{ra}	– front and rear axle equivalent shock-absorber damping, [Nsm^{-1}]	m_d	– mass of the driver, [kg]
b_{fb}, b_{rt}	– equivalent tyre damping for the front and the rear axle, [Nsm^{-1}]	m_{fa}, m_{ra}	– front and rear axle mass, [kg]
b_s	– shock-absorber damping of the driver seat suspension system, [Nsm^{-1}]	m_s	– mass of the driver's seat, [kg]
b_{t1}	– single tyre damping on the front and the rear axle, [Nsm^{-1}]	RMS	– root mean square, [–]
c_1, c_2	– front and rear axle single air bag stiffness, [Nm^{-1}]	V	– vehicle speed, [ms^{-1}]
c_c	– seat cushion stiffness, [Nm^{-1}]	z	– vertical movement of the center of gravity, [m]
CF	– crest factor, [–]	z_d	– vertical movement of the driver, [m]
c_{fa}, c_{ra}	– front and rear axle equivalent air bags stiffness, [Nm^{-1}]	$Z_{\text{din,eff}}$	– RMS value of dynamic axle load, [N]
c_{fb}, c_{rt}	– equivalent tyre stiffness for the front and the rear axle, [Nsm^{-1}]	$Z_{\text{dyn}}(t)$	– dynamic axle load, [N]
c_s	– spring stiffness of the driver seat suspension system, [Nm^{-1}]	z_{fa}, z_{ra}	– vertical movement of the front and the rear axle, [m]
c_{t1}	– single tyre stiffness on the front and the rear axle, [Nm^{-1}]	Z_{max}	– maximal value of the total axle load, [N]
d	– distance from the driver seat to center of gravity of loaded bus, [m]	z_s	– vertical movement of the seat, [m]
DLC	– dynamic load coefficient, [–]	Z_{st}	– static axle load, [N]
f	– road excitation frequency, [Hz]		
IRI	– international roughness index, [mkm^{-1}]		
		Greek symbols	
		θ	– pitching, [rad]
		λ	– irregularities wavelength, [m]
		ζ_1, ζ_2	– road roughness on the bus front and rear wheels, [m]
		σ_z	– standard deviation of total axle load [N]
		Acronyms	
		DWL	– dynamic wheel load
		PSD	– power spectral densities

References

- [1] Stokić, M., Vujanović, D., Vehicle Procurement Criteria Evaluation, *Proceedings*, 4th Interantional Conference on Traffic and Transport Engineering, Belgrade, Serbia, 2018, pp. 407-415
- [2] Riener, A., *et al.*, Subliminal Vibro-Tactile Based Notification of CO₂ Economy While Driving, *Proceedings*, 2nd International Conference on Automotive User Interfaces and Interactive Vehicular Applications, Pittsburgh, Penn., USA, 2010, pp. 92-101
- [3] Descornet, G., Road-Surface Influence on Tire Rolling Resistance, in: *Surface Characteristics of Roadways*, (Eds. Meyer, W., Reichert, J.), International Research and Technologies, West Conshohocken, Penn., USA, 1990, pp. 401-415
- [4] Van Dam, T. J., *et al.*, Towards Sustainable Pavement Systems: a Reference Document (No. FHWA-HIF-15-002), Federal Highway Administration, Washington, D. C., USA, 2015
- [5] Zaabar, I., Chatti, K., Calibration of HDM-4 Models for Estimating the Effect of Pavement Roughness on Fuel Consumption for US Conditions, *Transportation Research Record*, 2155 (2010), 1, pp. 105-116
- [6] Ivkovic, I., *et al.*, Influence of Road and Traffic Conditions on Fuel Consumption and Fuel Cost for Different Bus Technologies, *Thermal Science*, 21 (2017), 1B, pp. 693-706
- [7] Potter, T. E. C., *et al.*, Road-Damaging Potential of Measured Dynamic Tyre Forces in Mixed Traffic, Proceedings of the Institution of Mechanical Engineers – Part D: *Journal of Automobile Engineering*, 210 (1996), 3, pp. 215-225

- [8] Cebon, D., Interaction Between Heavy Vehicles and Roads, Report No. SP-951, Cambridge University, Cambridge, UK, 1993
- [9] Kenis, W. J., et al., Spatial Repeatability of Dynamic Wheel Loads for Heavy Vehicles: a Literature Review, *International Journal of Heavy Vehicle Systems*, 5 (1998), 2, pp. 116-148
- [10] Agostinacchio, M., et al., The Vibrations Induced by Surface Irregularities in Road Pavements – A Matlab® Approach, *European Transport Research Review*, 6 (2014), 3, pp. 267-275
- [11] Xia, R., et al., Effect Analysis of Vehicle System Parameters on Dynamic Response of Pavement, *Mathematical Problems in Engineering*, 2015 (2015), ID 561478
- [12] Gillespie, T., et al., Effects of Heavy Vehicle Characteristics on Pavement Response and Performance, Final Report No. UMTRI 92-2, University of Michigan, Ann Arbor, Mich., USA, 1992
- [13] Nijemčević, S., et al., *Tehnička knjiga* (Technical Book) (in Serbian), Ikarbus AD, Belgrade, Serbia, 2001
- [14] Mladenović, D., Bus Dynamic Behaviour in Real Driving Conditions (in Serbian), Ph. D. thesis, University of Belgrade, Belgrade, Serbia, 2008
- [15] Sekulić, D., Investigation of Passengers' Oscillatory Comfort in the Bus with Respect to the Seat Position and Quality (in Serbian), Ph. D. thesis, University of Belgrade, Belgrade, Serbia, 2013
- [16] Etefagh, M. M., et al., Reliability Analysis of the Bridge Dynamic Response in a Stochastic Vehicle-Bridge Interaction, *KSCE Journal of Civil Engineering*, 19 (2015), 1, pp. 220-232
- [17] Kim, R. E., et al., Stochastic Analysis of Energy Dissipation of a Half-Car Model on Non-Deformable Rough Pavement, *Journal of Transportation Engineering – Part B: Pavements*, 143 (2017), 4, pp. 1-10
- [18] Demić, M., Diligenski, Dj., Numerical Simulation of Shock Absorbers Heat Load For Semi-Active Vehicle Suspension System, *Thermal Science*, 20 (2016), 5, pp. 1725-1739
- [19] ***, University of Michigan, RoadRuf User Reference Manual, 2016, www.pathwayservices.com
- [20] Simić, D., *Dinamika Motornih Vozila: Oscilacije i Vešanje Automobila* (Motor Vehicle Dynamics-Oscillation and Vehicle Suspension – in Serbian), University of Kragujevac, Kragujevac, Serbia, 1975
- [21] ***, The Transtec Group, ProVAL User's Guide-Version 3.6, 2016, <http://www.roadprofile.com>
- [22] ***, ISO 2631, Mechanical Vibration and Shock-Evaluation of Human Exposure to Whole-Body Vibration, 1997, <https://www.iso.org/standard/7612.html>
- [23] Cole, D. J., Cebon, D., Truck Suspension Design to Minimise Road Damage, Proceedings of the Institution of Mechanical Engineers – Part D: *Journal of Automobile Engineering*, 210 (1996), 2, pp. 95-107
- [24] Gillespie, T., *Fundamentals of Vehicle Dynamics*, SAE, Warrendale, Penn., USA, 1992